



## Microstructural and Mechanical Properties of Sono-Ormosils

E. BLANCO

*Departamento de Física de la Materia Condensada, Universidad de Cádiz, Apartado 40, 11510-Puerto Real, Cádiz, Spain*

M. GARCÍA-HERNÁNDEZ AND R. JIMÉNEZ-RIOBÓO

*Instituto de Ciencia de Materiales de Madrid, C.S.I.C., Cantoblanco, E-28049-Madrid, Spain*

R. LITRÁN

*Departamento de Física de la Materia Condensada, Universidad de Cádiz, Apartado 40, 11510-Puerto Real, Cádiz, Spain*

C. PRIETO

*Instituto de Ciencia de Materiales de Madrid, C.S.I.C., Cantoblanco, E-28049-Madrid, Spain*

M. RAMÍREZ-DEL-SOLAR

*Departamento de Física de la Materia Condensada, Universidad de Cádiz, Apartado 40, 11510-Puerto Real, Cádiz, Spain*

**Abstract.** Monolithic pieces and films of ormosils were obtained from ultrasound-assisted polycondensation of tetraethoxysilane (TEOS) and polydimethylsiloxane (PDMS). These sono-ormosils were studied by means of high resolution Brillouin spectroscopy and their textures analyzed from adsorption isotherms. Evidence is given for the occurrence of organic and inorganic micro-phase separation in samples with high polymer concentrations. Nitrogen isotherms show that the texture of the samples is highly dependent on the composition.

**Keywords:** sono-ormosil, textural features, Brillouin spectroscopy, microstructural model

### 1. Introduction

In recent years, sol-gel scientists have dedicated a huge effort to study the unique properties of organically modified silicates (ormosils) [1, 2]. A full exploitation of the mechanical properties of these materials requires a deep understanding of the interplay between structural and dynamical correlations. However, investigations have been mainly focused on the macroscopic elastic features [3, 4] with little attention paid to their correlation with the dynamical elastic behavior. In this context, we have made

use of Brillouin scattering which has been widely proven to be an essential technique in determining the relationship between structure and elastic properties [5].

Ormosils studied in this paper were prepared by the solventless sonogel route [6, 7] in order to extend the compositional range in which no microphase separation occurs [4, 8–10]. Elasticity results are correlated with the textural analyses performed on samples with different organic-inorganic ratios and the overall information is explained using a simple microstructural picture of the sono-ormosils network.

## 2. Experimental

Ormosils have been prepared by a solventless sol-gel route using tetraethoxysilane (TEOS) from Merck as inorganic precursor and polydimethylsiloxane (PDMS) from Hüls America Inc., with an average molecular weight of 550, as organic source. Hydrolysis and condensation reactions were carried out in an acid environment and promoted by a high power ultrasound probe (20 kHz, 15 W) [6].

In order to promote the copolycondensation reaction against self-polymerization of PDMS [7], samples were prepared as follow. First, TEOS-acidic water mixtures (2 mol H<sub>2</sub>O/mol TEOS) were subjected to ultrasound radiation ( $E_s = 60 \text{ J} \cdot \text{cm}^{-3}$ ). Then, amounts of PDMS, ranging from 0 to 40 wt%, referred to TEOS were added, and, finally, the mixtures were subjected to an additional ultrasonic dose to complete a total energy dose of  $0.12 \text{ kJ} \cdot \text{cm}^{-3}$ . The resulting transparent sols were poured into a plastic container and left to gel. After one week ageing and two weeks drying at room temperature, monolithic pieces of dried ormosils resulted. These were transparent for lower doses of organic component, but became milky for the highest dose.

Thick film samples of the same compositions were also prepared by deposition of the sols in a silicon rubber cell, obtaining free standing films of about  $10 \mu\text{m}$  of thickness with plane parallel faces and transparency suitable for Brillouin spectroscopy [11].

For the sake of clarity, the organic fraction in the hybrid material will be expressed in the following as monomer molar fraction, that is:  $X = \text{DMS mol}/(\text{TEOS mol} + \text{DMS mol})$ ,  $X$  being 0.24, 0.41, 0.55 and 0.65 in the samples studied.

Pore size distribution, specific surface area [12] and porous volume, have been evaluated from nitrogen adsorption isotherms, performed in a Sorptomatic 1990 FISON equipment. Samples were previously evacuated, using a rotary pump, in order to remove the liquid from the pores. Complete adsorption-desorption isotherms were analyzed and pore size distributions were evaluated using the Horvath/Kawazoe method [13].

The density of the samples was estimated by pycnometry using two different probes. Thus, bulk density was measured by the Archimedes method using cyclohexane ( $\rho = 0.78 \text{ g} \cdot \text{cm}^{-3}$ ), with negligible penetration into the pores. The density of the solid organic-inorganic network (skeletal density) was estimated from helium pycnometry.

The elasticity of materials was evaluated by Brillouin spectroscopy [14], performed with two different geometries: the backscattering ( $180^\circ$ ) and the special  $90^\circ$  scattering geometry [15]. The corresponding phonon wavelengths are:  $\Lambda^{90^\circ} = \lambda_0/\sqrt{2}$  and  $\Lambda^{180^\circ} = \lambda_0/2n$ , where  $\lambda_0$  is the wavelength of the light source (514.5 nm), and  $n$  is the relevant refractive index of the sample. The elastic constant is derived from the spectra using:  $c = \rho \cdot v^2$ , where  $\rho$  is the density of the material and the sound velocity,  $v = f \cdot \Lambda$ ,  $f$  being the corresponding Brillouin shift in frequency units. For our acoustic isotropic system there are only two independent elastic constants,  $c_{11}$  and  $c_{44}$ , corresponding to the longitudinal and shear polarized modes, respectively [16].

## 3. Results and Discussion

Textural features of the samples were inferred from the nitrogen physical adsorption on the free surface of the samples, at the liquid nitrogen temperature. On the basis of initial experiments, all the samples were previously evacuated at  $60^\circ\text{C}$ . The choice of this relatively low temperature, has been made in order to remove the residues from the pore walls, without noticeable changes in the textural features of the hybrid material. Adsorption-desorption isotherms for sonoormosils with different DMS concentrations are shown in Fig. 1. Isotherms corresponding to the 0.24 and 0.41 DMS samples can be considered as IUPAC type I [17], characteristic of microporous solids. Both curves show that pore filling takes place at low relative pressure, above which a plateau occurs, indicating little additional adsorption. Nevertheless, for the isotherm corresponding to 0.55 of PDMS ormosil, the shape is much closer to those produced by adsorption on mesoporous materials, a type IV isotherm, with a hysteresis loop due to capillary condensation in the mesopores. Finally, the curve shape for the 0.65 DMS sample can be attributed to a macroporous network, where the absence of small pores in the sample causes no adsorption at low pressures.

Similar trends are found from the textural parameters derived from these experiments (Table 1). The main feature is that the surface area drastically decreases once the organic phase becomes the major component in the sample. Additional information about the influence of organic phase on the solid network can be inferred from the volume/surface ratio. The increase of this parameter with DMS concentration points to an

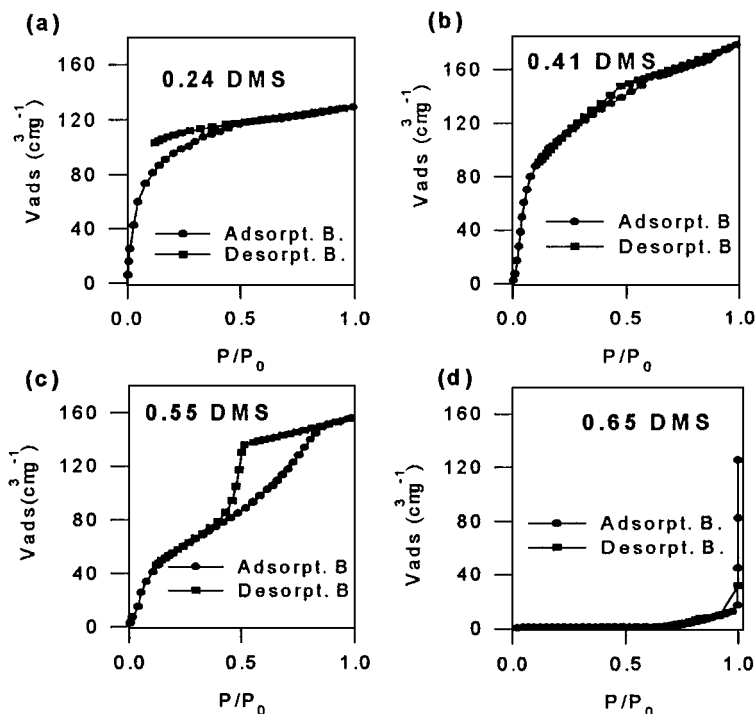


Figure 1. Adsorption-desorption isotherms for ormosils with different DMS molar concentrations, performed after samples were evacuated at 60°C.

enlargement of the pores. As noted previously, the highest DMS concentration studied ( $X = 0.65$ ) leads to a hybrid network without noticeable porosity at the resolution level of the experiment. The BET method is not valid to estimate a specific surface value in this case where there is not adsorption at low relative pressure. It is important to notice that the density of the 0.65 sample, measured by He and  $C_6H_{12}$  pycnometries, is not significantly different (Table 1), supporting the absence of mesopores in this sample.

Table 1. Sono-ormosil textural parameters, obtained from nitrogen adsorption isotherms, and He and  $C_6H_{12}$  pycnometry, for samples with different DMS concentration ( $S_{BET}$ , surface area;  $V_p$ , pore volume).

$X$ DMS	Bulk density ( $g \cdot cm^{-3}$ )	Skeletal density ( $g \cdot cm^{-3}$ )	$S_{BET}$ ( $m^2 \cdot g^{-1}$ )	$V_p$ ( $cm^3 \cdot g^{-1}$ )
0.24	1.39	1.45	350	0.20
0.40	1.14	1.32	372	0.27
0.55	1.07	1.18	220	0.24
0.65	~1.17	1.17	—	0.018

Pore size distributions corresponding to these four samples are shown in Fig. 2. The contribution of small pores to the total pore volume becomes lower as the PDMS concentration is increased, especially for the

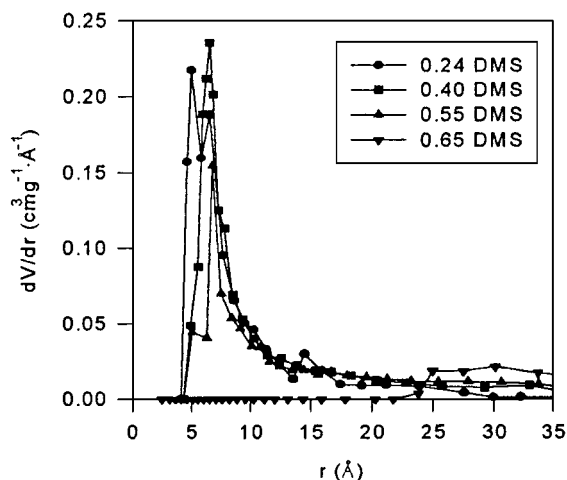


Figure 2. Pore size distributions obtained from the adsorption branch of the isotherms presented in Fig. 1. Notice that increasing the DMS concentration modifies the ormosil pore size distribution.

$X = 0.55$  and  $X = 0.65$  DMS samples. In the latter, there are no pores with radius smaller than 25 Å.

From the analysis of the Brillouin spectra, valuable information about the influence of DMS content on the static and dynamic elastic properties is obtained (Fig. 3) [16]. The elastic constants were evaluated, from Brillouin shifts and bulk densities, for monolithic or thick film samples. As no transverse modes were noticeable from the spectra, probably because they are severely damped in these porous materials, only  $c_{11}$  values are presented in Fig. 3(a). The figure reveals a smooth decrease of the elastic constant with increasing DMS concentration, without any significant influence from the sample morphology. Calculated values tend asymptotically to the value for the pure PDMS (liquid), reaching this at a concentration close to 0.40. This indicates the influence of the polymeric phase concentration on the elastic properties of sono-ormosils.

A reliable estimation of the hypersonic attenuation ( $\Gamma$ ) was obtained from the half width at half maximum

(HWHM) of the Brillouin peaks, corrected for the Rayleigh value (Fig. 3(b)). The change of the DMS concentration dependence of the hypersonic attenuation should be noted, initially decreasing until a minimum is reached at about  $X = 0.4$ , and increasing for higher concentrations. Considering the inverse relation between the hypersonic attenuation and the phonon lifetime, it is possible to explain the attenuation behavior in terms of a changing number of interfaces in the medium (i.e., pores and segregated microphases). Thus, for low PDMS concentration, the organic phase links uniformly to the inorganic phase, leading to a homogeneous hybrid organic-inorganic network. The enrichment in DMS content of the solid network together with the increase in the average pore size, as demonstrated from the adsorption experiments, would lead to a reduction in the number of interfaces, which explains the hypersonic attenuation decay. However, it seems to be a limiting DMS concentration ( $X \approx 0.4-0.5$ ) above which some polymer tends to adopt a globular form, leading to microphase separation and, consequently, increasing the attenuation.

This interpretation of the elastic data in terms of two coexisting morphologies of PDMS (segment-like and globular) are clearly supported by previous NMR results. Evaluation of the optical properties points out that the refractive index is also sensitive to the existence of a characteristic DMS concentration [16].

The observed elastic behavior can be qualitatively explained in terms of a simple model based on those used by Mackenzie [3]. In agreement with our results, the model is based on the assumption of two different microstructures for PDMS, a segment-like configuration within the backbone of the sonogel network and a quasiglobular (liquid-like) configuration. Both forms are parallel branched while being branched in series to the silica structure. Normalizing their relative contributions to the sample elastic behavior according to the composition  $x$ , we obtain:

$$c_{11} = \frac{1}{\left(\frac{1-x}{c_1} + \frac{x}{c_2(1-x) + c_3x}\right)} \quad (1)$$

where  $c_2$  and  $c_3$  are the elastic constants of PDMS in a segment-like and globular-like configuration, respectively, and  $c_1$  is the elastic constant of the sonogel. Using the elastic constant of liquid PDMS for  $c_3$ , an estimation of  $c_1$  and  $c_2$  is obtained by fitting Eq. (1) to the experimental results. The continuous line in Fig. 3, corresponding to the best fit ( $c_1 = 17$  GPa,  $c_2 = 3$  GPa),

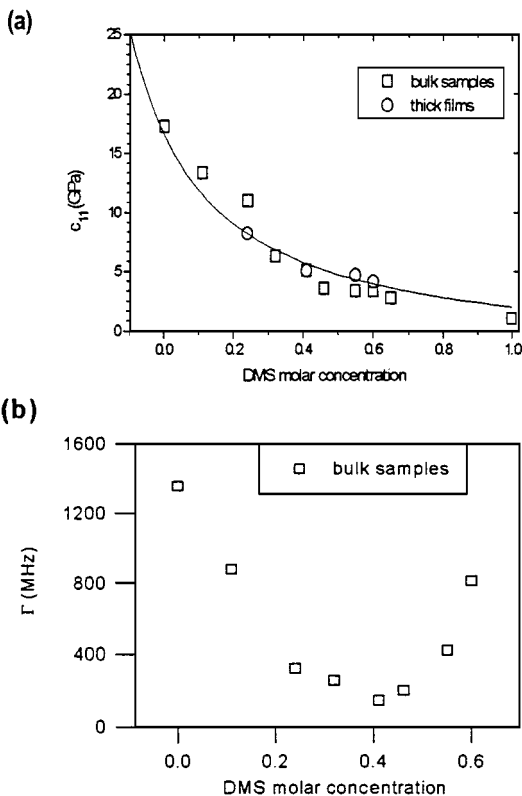


Figure 3. DMS concentration dependence of the longitudinal elastic constant (a) and the hypersonic attenuation (b). In both cases, a change in these parameters can be observed, for DMS concentrations higher than 0.40–0.50.

indicates that the model provides a semiquantitative description of the elastic behavior of the sonogels.

#### 4. Conclusions

High resolution Brillouin spectroscopy and nitrogen adsorption have been used to investigate the elastic and textural properties of ormosils obtained by the sonogel method. These techniques allowed the evaluation of the DMS concentration effect on the elastic constant,  $c_{11}$ , the hypersonic attenuation,  $\Gamma$ , and pore size distribution. No appreciable difference in behavior between monolithic and film samples was observed. The concentration dependence of both the static and dynamic elastic parameters markedly changed around 0.4–0.5 DMS.

The inclusion of the polymeric phase in the sonogel network modifies the textural characteristics of these samples, increasing the pore size average and giving rise to microphase segregation when it reaches 50%.

A model, assuming two different configurations for the polymer, shows good agreement with the experimental results and supplies, as fitting parameters, the elastic constants of the sonogel backbone and that of the polymer embedded in it.

#### Acknowledgments

This work was supported by the CICYT (Proj. MAT-95-0040-C02-02) and Junta de Andalucía (TEP0015).

#### References

1. G. Philipp and H. Schmidt, *J. Non-Cryst. Solids* **63**, 283 (1984).
2. G.L. Wilkes, B. Orlor, and H.H. Husng, *Poly. Prep.* **26**, 300 (1985).
3. Y. Hu and J.D. Mackenzie, *J. Mat. Sci.* **27**, 4415 (1992) and references therein.
4. T. Iwamoto and J.D. Mackenzie, *J. Sol-Gel Sci. Tech.* **4**, 141 (1995).
5. J. Kruger, in *Optical Techniques to Characterize Polymer Systems*, edited by H. Bassler (Elsevier, Amsterdam, 1989), p. 429.
6. L. Esquivias and J. Zarzycki, in *Ultrastructure Processing of Advanced Ceramics*, edited by J.D. Mackenzie and D.R. Ulrich (Wiley, New York, 1987), p. 255.
7. M. Ramírez-del-Solar, L. Esquivias, A.F. Craievich, and J. Zarzycki, *J. Non-Cryst. Solids* **147/148**, 206 (1992).
8. H. Huang, B. Orlor, and G.L. Wilkes, *Macromolecules* **20**, 1322 (1987).
9. T. Iwamoto, K. Morita, and J.D. Mackenzie, *J. Non-Cryst. Solids* **159**, 65 (1993).
10. K. Morita, Y. Hu, and J.D. Mackenzie, *J. Sol-Gel Sci. Tech.* **3**, 109 (1994).
11. M. García-Hernández, R.J. Jiménez-Riobóo, C. Prieto, J.J. Fuentes-Gallego, E. Blanco, and M. Ramírez-del-Solar, *Appl. Phys. Lett.* **69**, 3827 (1996).
12. S. Brunauer, P.H. Emmett, and E. Teller, *J. Amer. Chem. Soc.* **60**, 309 (1938).
13. G. Horwath and K. Kawazoe, *J. Chem. Eng. of Japan*, **16**(6), 470 (1983).
14. J.R. Sandereock, *Trends in Brillouin scattering, Topics in Applied Physics* (Springer, Berlin, 1982), Vol. 51, p. 173.
15. J.K. Krüger, A. Marx, L. Peetz, R. Roberts, and U.G. Unruh, *Col. Pol. Sci.* **264**, 403 (1986).
16. R.J. Jiménez-Riobóo, M. García-Hernández, C. Prieto, J.J. Fuentes-Gallego, E. Blanco, and M. Ramírez-del-Solar, *J. Appl. Phys.* **81**(12), (1997).
17. R.W. Sing and Members of the Subcommittee on Reporting Gas Adsorption Data, *Pure Appl. Chem.* **57**(4), 603 (1985).